PROCEEDINGS, 51st Workshop on Geothermal Reservoir Engineering
Stanford University, Stanford, California, February 9-11, 2026
SGP-TR-230

Numerical Modeling to Investigate Geothermal Power Production and Lithium Co-Extraction in the Great Salt Lake Desert

Hannah S. Gatz-Miller[1], Petra M. Peirce[2], Jennifer M. Frederick[1], Carolina Muñoz-Saez[2], Franek Hasiuk[1]

[1]Sandia National Laboratories, Albuquerque, NM

[2]Cornell University, Ithaca, NY

hsgatzm@sandia.gov

Keywords: Critical minerals, lithium, modeling

ABSTRACT

Wendover Graben in the Great Salt Lake Desert (GSLD), Utah, has been identified as a potential resource of both geothermal energy and lithium (Li^+) extraction. Facilities capable of Li^+ removal constructed as part of a geothermal power plant could increase Li^+ availability and improve costs associated with both geothermal and Li^+ extraction. Previous work on Wendover Graben has suggested a high geothermal gradient and reservoir temperature greater than 200°C, facilitated by circulation of hot water through faults from deeper, carbonate and sandstone aquifers (~7000 m thick), through a thin volcanic and tuff layer (100-400 m thick) up to shallower aquifers (~200-1,200 m thick) in the uppermost basin fill. Well data suggests aqueous Li^+ concentration below 10 m depth in the basin fill aquifer approximately 17 ppm, and up to 41 ppm in the shallow brine (above 10 m depth). To investigate the potential for combining geothermal energy and Li^+ extraction, a series of reactive transport models of Wendover Graben, parameterized using available data in the literature, were constructed in the reactive-transport code PFLOTRAN.

Simulation results indicate that Li^+ from dissolution of Li-bearing igneous minerals can be transported along with deep, hot water via faults to the basin fill aquifer, facilitating both increased Li^+ concentration and precipitation of Li^+ bearing clays at shallower depths. These results suggest a potential mechanism by which both increased Li^+ concentration and hot (>200°C) water can be found at depths reasonable for well construction and geothermal power production. This supports the need for additional work to investigate Wendover Graben hydrogeology and mineralogy to improve model parameterization and further determine the location's suitability for geothermal power production and potential co-extraction of dissolved Li^+.

1. INTRODUCTION

1.1 Geothermal and Lithium Background

The search for new sources of critical minerals such as lithium (Li^+), for battery components and other aspects of power storage and production, is inextricably intertwined with increased energy needs (Mends and Chu, 2023; Zhou et al., 2025, p. 202). Originating from igneous material (Jancsek et al., 2023; Zhou et al., 2025) aqueous Li^+ may also precipitate (as well as later re-dissolve) as a component of clay deposits (Benson et al., 2023; Decarreau et al., 2012), such as in the McDermitt Caldera (Glanzman et al., 1978), or remain as an aqueous component of subsurface brines (Lee et al., 2024; Mends and Chu, 2023; Stringfellow and Dobson, 2021), such as in the Salton Sea (Dobson et al., 2023). In the past, Li^+ has been extracted either from vast, often environmentally hazardous evaporation ponds where aqueous Li^+ has collected over geologic timescale in closed basins, or has been mined directly from Li^+ bearing rocks such as pegmatites (Mends and Chu, 2023; Zhou et al., 2025). To access Li^+ stored in deep subsurface brines would incur high pumping and extraction costs (Mends and Chu, 2023; Stringfellow and Dobson, 2021; Warren, 2021). However, removal of Li^+ from brines already being pumped to the surface for other purposes, such as geothermal heat mining, may provide a new source of Li^+ in addition to reducing operational costs. This approach has been suggested for example, for the well-known Salton Sea in California, a unique confluence of geothermal operations and rich brines (Dobson et al., 2023; Warren, 2021). However, the unique geologic circumstance of the Salton Sea make Li^+ separation and extraction increasingly- energy intensive and expensive, particularly when dealing with highly concentrated brines that also contain high concentrations of elements with similar chemical reactivity to Li^+, such as magnesium (Mends and Chu, 2023). Here, we investigate the potential for co-extraction of Li^+ and geothermal heat from brines with reported Li^+ concentrations that may still be economically worthwhile to extract as part of a co-operation with a geothermal plant, from comparatively dilute brines that may be found more frequently in the subsurface.

To investigate this possibility, Wendover Graben in the Great Salt Lake Desert (fig. 1) was identified as a location of interest due to reported Li^+ concentrations up to 17 ppm in deeper (>10 m) and 41 ppm in shallower (< 10 m) sodium chloride (NaCl) dominant brines, together with reservoir temperatures greater than 200°C (Goode, 1978; Smith et al., 2011; Turk et al., 1973). A conceptual model of the hydrogeologic system was constructed using available data in the literature and then implemented in a series of flow and reactive-transport simulations using PFLOTRAN, a massively parallel, open-source reactive transport simulator (Hammond et al., 2014; Lichtner et al., 2015).

1.2 Wendover Graben Geology

Wendover Graben is made up of a series of normal faults and basin fill formed as a part of the Basin and Range extensional province (Goode, 1978; Smith et al., 2011; Sweetkind et al., 2011a). It is located to the far west of the Great Salt Lake Desert, close to the Utah-Nevada border, and the town of Wendover (Figure 1). At the macro scale of the Basin and Range, the shallowest layers consist of coarse-grained basin fill deposits of up to 1,000 m thickness overlying a thin igneous unit (approximately 100-300 m thick of lava and tuff), overlying a carbonate and sandstone aquifer up to 7,000 m thick. Below the carbonate aquifer is a siliciclastic confining unit (~1,500 m thick), followed by a lower carbonate aquifer (up to 5,000 m thick), and basement (siliciclastic sedimentary and metamorphic rocks) (Sweetkind et al. 2011a, b;) (Table 1). For Wendover Graben, significant concentrations of Li^+ (15-41 ppm) have been reported only in the uppermost layers of the basin fill (Turk et al., 1973). The thin crust and warm mantle have been suggested as the heat source for the Great Basin (Smith et al., 2011) and the mechanism for heat transport from the carbonate aquifer is via faults connecting the basin fill aquifer and the upper carbonate aquifer formed during basin extension (Smith et al., 2011). The faults are estimated to extend vertically between 300-1500 m (Kim, 1985; Smith et al. 2011). Faults in the western Basin and Range are suggested to have reactivated between 3 and 0.5 million years ago, with a vertical displacement rate of 1-2 mm/yr (Carena and Friedrich, 2018).

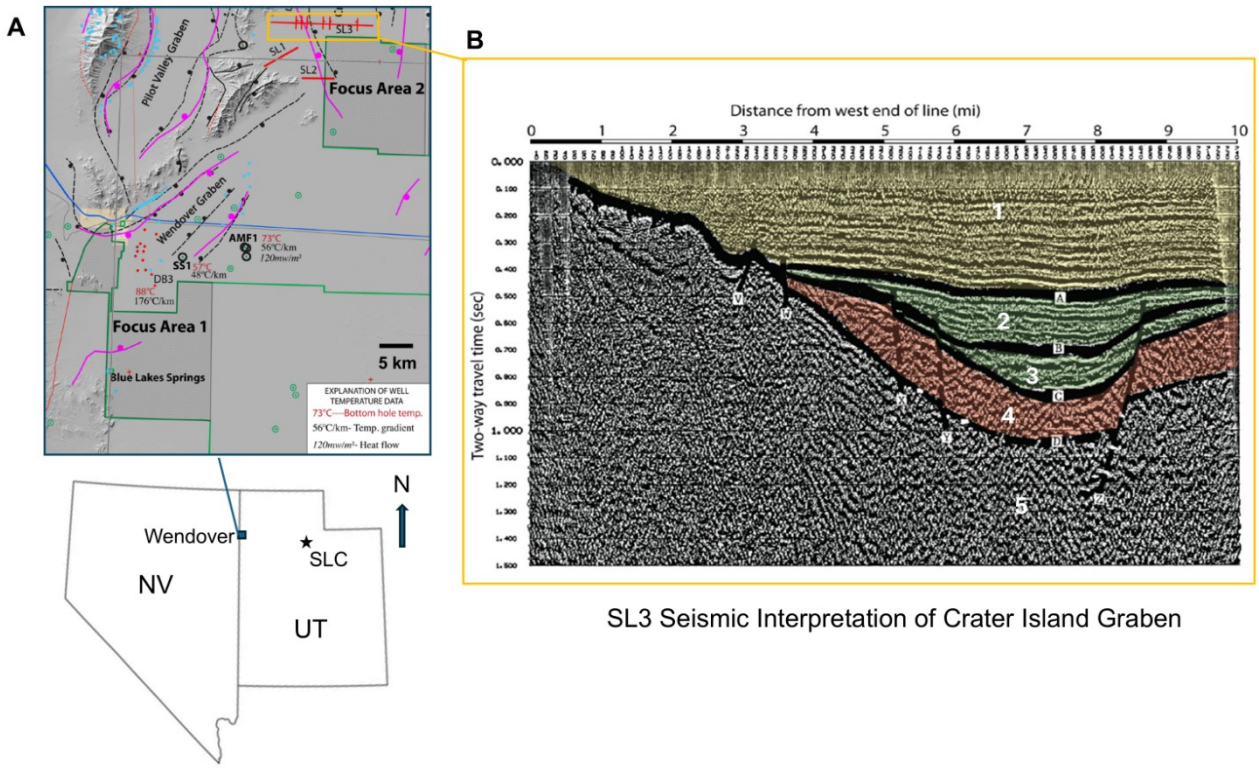

SL3 Seismic Interpretation of Crater Island Graben

Figure 1: Map of (A) Wendover Graben location modified from Smith et al. (2011) and (B) Seismic interpretation of nearby Crater Island Graben from Kim (1985) and (Smith et al., 2011). Graben fault bounds indicated with black (older) and pink (more recent), blue dots represent springs, green represent earthquake epicenters, red represent deep brine wells, and black circles represent oil wells. The three labeled wells are Deep Brine Well 3 (DB3), Shell Salduro #1 (SS1) and Alpha Minerals Federal #1 (AMF1) as well as their recorded bottom hole temperature, thermal gradient and heat flow. Focus areas refer to Utah Testing and training (UTTR) regions of interest for geothermal power production (Smith et al., 2011). Materials from the surface down are interpretated as 1) unconsolidated sediment (Pliocene), 2) and 3) limestones and interbedded shales (Miocene-Pliocene) 4) volcanics (Oligocene), 5) carbonates (Pennsylvanian) (Kim, 1985).

Table 1: Stratigraphic units of the Great Salt Lake Desert Area. Modified from Sweetkind et al. (2011b, a).

Unit	Description
Upper/Lower Basin Fill Aquifer Unit	Coarse-grained basin fill. Deep burial and cementation may reduce permeability. (Lower and upper units connected in GSL Desert Region). (Cenozoic).
Latite Lava, Tuffaceous Sandstone, and Tuff	Rhyolite-andesite, welded and nonwelded tuffs (caldera eruptions), basalt, andesite, rhyolite (lava flows). 100-3000 m. Fractured rocks can be flow zones for aquifer. (Cenozoic).

Upper Carbonate Aquifer Unit	Sandstone, carbonates. Carbonates associated with Ancestral Rocky Mountain orogeny. Upper Paleozoic (Pennsylvanian and Permian)
Upper Siliciclastic confining unit	Mudstone, siltstone sandstone deposited from high point related to Antler orogeny, lacks secondary (i.e., from dissolution or fractures) permeability. Upper Paleozoic (Mississippian shale).
Lower Carbonate Aquifer Unit	Cambrian-Devonian. Carbonate rocks and sandstone deposited in shallow waters, high permeability, has fracture permeability and networks, material eroded with changes to sea level. Lower Paleozoic (Cambrian – Devonian)
Non-Carbonate Confining Unit	Siliciclastic sedimentary rocks

The basin fill aquifer at Wendover Graben can be further subdivided into shallow and deep brine aquifers. The shallow brine aquifer is described (Turk et al., 1973) as the upper 7 m of lacustrine sediments, historically used for potash mining, with 45% porosity and a 1-2 m thick salt crust from historic Lake Bonneville evaporites overlaying the top of the unit. The geochemistry of the brine, obtained from shallow wells, indicates high (10^4 mg L^{-1}) Na^+ and Cl^- concentrations, and Li^+ concentration ranging from 15-41 mg L^{-1}. Recharge is from rainfall and well temperatures vary seasonally, ranging from 13°-25°C. Origin of the brine has been suggested as dissolution from clays, as well as evaporites deposited prior to Lake Bonneville (e.g., Turk et al. 1973). Brine concentration in the deep brine aquifer (Turk et al., 1973) is described as more dilute below 580 m. Drill logs describe clay and gypsum for the first ~200 m, before grading into sandy clay, gravel, and conglomerates, and eventually hitting black volcanic rock at approximately 400 m (Goode, 1978; Turk et al., 1973). Measured well temperatures ranged from 22°-88°C, with possible reservoir temperatures ranging from 177°-285°C (Goode, 1978; Turk et al., 1973). Hydraulic conductivity of the basin fill from pumping and other well tests was between the order of 2. x 10^{-6} m s^{-1} 2. x 10^{-5} m s^{-1} in the deep brine aquifer, and an order of magnitude lower in the shallow aquifer (Turk et al., 1973).

Over the several million years of basin formation, lithium-rich igneous material was likely extensively weathered, resulting in igneous material dissolution and precipitation of the lithium-rich secondary clay minerals suggested as one potential brine source, along with evaporation of Lake Bonneville and concentration of its mineral constituents. This process of aqueous lithium (Li^+) originating from igneous material and incorporating into clay weathering products has also been suggested as a mechanism behind high Li^+ concentrations (up to 0.65%) in clays in the McDermitt Caldera (Glanzman et al., 1978). The clays at McDermitt Caldera are described as hectorite, a Li^+ enriched variety of smectite, and illite, occurring in zones of volcanic glass and potassium-feldspar (Glanzman et al., 1978). Although clays are described in drill logs around Wendover Graben (e.g., Turk et al. 1973), clays are described mainly by color (blue, green, light brown), texture (sticky, calcareous) and mineralogy (if specified) as montmorillonite, kaolinite, and illite (Goode, 1978). Exact Li^+ content of the clays is unknown. Igneous material in well logs from Wendover Graben is described as a highly heterogeneous mix of volcanic breccia, tuff, andesite, basalt, and gabbro, containing pyroxene, hornblende, plagioclase feldspar, chlorite, serpentinite, olivine, amphibole, muscovite, and biotite, in addition to volcanic glass present in the tuff (Glanzman et al., 1978). While Li^+ bearing minerals in granite pegmatites used for traditional hard rock Li^+ extraction, such as lepidolite, zinnwaldite, and spodumene are not reported at Wendover Graben (Whelan and Petersen, 1976), other minerals such as biotite, muscovite, pyroxene, feldspar and chlorite which have been reported at Wendover Graben, are all Li^+ compatible, with chloritization of biotite suggested for high aqueous Li^+ concentration in geothermal waters reported in other regions (Jancsek et al. 2023; Repczynska et al. 2025).

2. METHODS

2.1 PFLOTRAN

Simulations were constructed and run using the reactive transport (RT) code PFLOTRAN. PFLOTRAN uses well-established governing equations to calculate coupled flow and transport through subsurface porous media in up to 3-dimensions (Hammond et al., 2014; Lichtner et al., 2015). For both fully and partially saturated conditions, PFLOTRAN can consider advective and diffusive transport, heat transport, and thermodynamic and kinetic processes, including intra-aqueous kinetic process and mineral processes (e.g., dissolution and precipitation) and resulting changes to permeability and porosity (Hammond et al., 2014; Lichtner et al., 2015). PFLOTRAN's new fracture process model (Frederick et al., 2025) was used to simulate subsurface fracture flow.

2.2 Conceptual Model

The literature-derived (e.g., Carena and Friedrich, 2018; Goode, 1978; Kim, 1985; Smith et al., 2011; Sweetkind et al., 2011b, 2011a; Turk et al., 1973), conceptual model of Wendover Graben (Figure 2) suggests upward movement of hot water from the deeper carbonate aquifer through faults into the basin fill. As hot water migrates towards the surface, Li^+ bearing materials in the igneous layer, such as volcanic glass and biotite dissolve, releasing Li^+ into solution. The dissolved Li^+ is then transported into the basin fill in the aqueous phase, or incorporated into Li^+ rich clays, potentially resulting in a subsurface zone with sufficient heat for geothermal power production, as well as an economically useful magnitude of aqueous Li^+.

2.3 Numerical Model Domain and Boundary Conditions

Simulations were parameterized using hydrogeological data from the literature available for the Great Salt Lake Desert, the Basin and Range region, and any publicly available data specific to Wendover Graben (Carena and Friedrich, 2018; Goode, 1978; Kim, 1985; Smith et al., 2011; Sweetkind et al., 2011b, 2011a; Thomas et al., 1986; Turk et al., 1973; Whelan and Petersen, 1976), to constrain model domain and boundary conditions for flow and geochemistry (Figure 2). An initial 2-dimensional fluid and heat flow model across the entire graben (Model A) was run for 2 million years to determine if flow through the graben's faults could reasonably move heat useful for geothermal power production from the deep carbonate aquifer to the basin fill (Figure 2 and 3). The 2-dimensional model results were then used to parameterize boundary and initial conditions for a zoomed-in 3-dimensional simulation (Model B) focused on a fracture-pair towards the east side of the graben. Geochemistry and later a set of injection and production wells were added to the zoomed simulation to determine magnitude and location of Li^+ dissolution over the million-year timescale, as well as potential for Li^+ extraction over thirty years of geothermal power production.

2.4 Model A. 2-D Flow Model

For the 2D flow model (Figure 2 and 3), the model domain extended 20,000 m in the x-direction, 7,700 m in the vertical direction, and 200 m in the y-direction, perpendicular to the Wendover Graben. A no-flow boundary was applied at the base and hydrostatic pressure boundaries were applied on the surface, east, and west sides, with pressure calculated with depth by PFLOTRAN given hydraulic head values of approximately 1,310 m to the west and 1276 m to the east based on potentiometric surface maps of the area (Thomas et al., 1986). A thermal gradient of 45°C km^{-1} was applied as an intermediate between suggested bounds of 35° - 60°C km^{-1} (Smith et al., 2011).

The model domain was set between -6,500 m to 1,200 m mean sea level (MSL), with the impermeable base representing the boundary between the Siliciclastic Confining Unit and the Carbonate Aquifer (Sweetkind et al., 2011a). A 6,000 – 7,000 m tick unit of higher permeability carbonate material was overlain by 400 m of igneous material, and then 500–1000 m of basin fill. An initial simulation without faults achieved horizontal flow from west to east and limited vertical flow. Following, four nearly vertical faults with aperture width of 3.0 x 10^{-4} m and extent of 2,000 m were placed at 3,100 m, 5,100 m, 8,100 m, and 1,100 m distance from the western boundary, based on fault orientation in the nearby Crater Island Graben (Kim, 1985, p. 198) (Figure 1). Aperture width was varied within reasonable range (Carena and Friedrich, 2018; Forbes et al., 2019) to facilitate vertical flow between hydrogeologic strata. Grid cells were 200 m x 200 m x 200 m (Figure 3). Simulations were run for 2 million years.

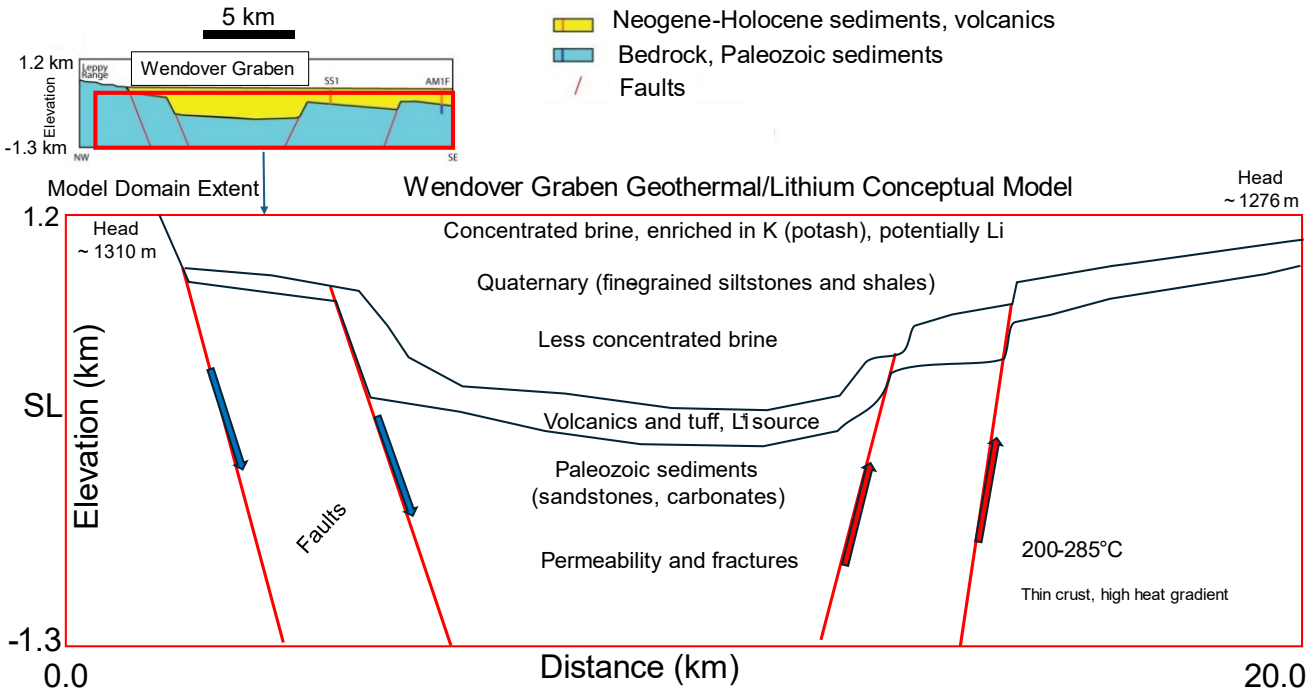

Figure 2: Conceptual model of flow and heat transport in the Wendover Graben, and potential processes contributing to Li^+ accumulation. Modified from Smith et al. (2011). Oil wells Shell Salduro #1 (SS1) and Alpha Minerals Federal #1 (AMF) shown on the east side of the graben. Blue arrows indicate potential downward flow of cool water along faults (red lines), and red arrows upward flow of hot water along faults.

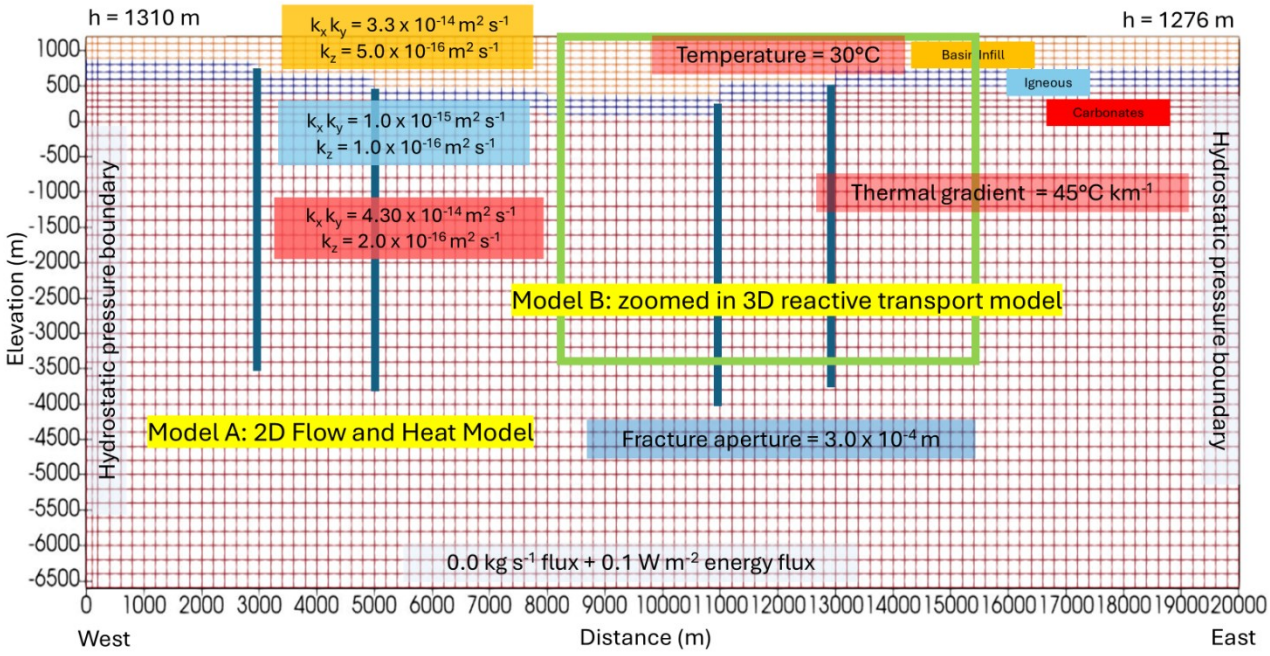

Figure 3. PFLOTRAN model domains for flow and heat transport simulations. The zone inside the green rectangle shows the bounds of the zoomed reactive transport model (Model B).

2.5 Model B. 3-D Reactive Transport Model

The 3-dimensional (3D) simulation zooms in on the eastern half of the graben (Figure 3, Figure 4), where results from the 2-D flow and heat transport simulation (Model A) indicated upward heat flow through the faults and accumulation of heat in the basin fill. Flow and heat boundary conditions for the 3-dimensional domain were taken from 2-D model results and used to parameterize hydrostatic boundaries and temperature of the front, back, east, west, and surface of the model domain. The base of the model was set at 3,500 m below MSL, and a flux of 1.0 x 10^{-8} m s^{-1} and 0.055 W m^{-2} was applied at the base between the distance of 10,000 m and 12,000 m to replicate observed vertical flow through the far eastern fault from Model A. After a flow and heat regime similar to that observed in Model A was established in Model B, a geochemical reaction network consisting of mineralogy and aqueous components reported present at Wendover Graben and the Great Salt Lake Desert from the literature (e.g. Goode, 1978; Kim, 1985; Sweetkind et al., 2011a; Turk et al., 1973) was added to Model B for reactive transport.

For reactive minerals, the carbonate aquifer was assumed to contain a mixture of 0.4 volume fraction quartz, 0.4 calcite, 0.02 albite and 0.02 potassium feldspar (0.16 porosity). The basin fill layer was assigned 0.2 volume fraction quartz, 0.5 albite, 0.15 potassium-feldspar, 0.05 calcite (0.1 porosity). For the igneous layer between the carbonate aquifer and the basin fill, initial mineralogy included quartz (0.25), enstatite (0.1), albite (0.3), potassium-feldspar (0.2), and Li-bearing biotite (0.1), while chlorite, Li-bearing chlorite, kaolinite, muscovite, Li-bearing muscovite, halite, and calcite were allowed to form if conditions permitted. Aside from pH and HCO_3^- which were constrained explicitly, initial concentration of aqueous components was set on the order of 10^{-8} mol L^{-1}, allowed to move towards equilibrium concentrations as the simulation progressed. HCO_3^- concentration in the basin bill was constrained by atmospheric concentrations of CO_2 gas at the top boundary, and initial pH was set as 7.0 (Goode, 1978; Turk et al., 1973). Biotite was selected as representative initial "Li-bearing initial igneous material', chlorite as a representative secondary "Li-bearing clay", and muscovite as a secondary potential mineral for Li^+ incorporation, with 0.26 mol Li^+ per mol biotite ($KFeMg_{0.87}Li_{0.26}(AlSi_3O_{10})(OH)_2$), 0.05 mol Li^+ per mol chlorite, and 0.12 mol Li^+ per mol muscovite (Eggleton and Banfield, 1985; Repczynska et al., 2025).

No biotite was assigned to the basin fill to ascertain if Li^+ that dissolved into solution from minerals in the igneous layer could migrate to the basin fill, or if a mineral source in the basin fill layer would be needed. Temperature and pH dependent kinetic rate constants were assigned from Palandri and Kharaka, (2004), and Smith and Carroll (2016) (Table 2). The PFLOTRAN Geothermal High Pressure, High Temperature database was used for thermodynamic properties (Lichtner et al. 2015). Simulation B was run for 1 million years.

Table 2: Kinetic rate parameters for active minerals from the literature ([1]Palandri and Kharaka, 2004; [2]Smith and Carroll, 2016) used for neutral, acidic and basic rate mechanisms.

Mineral	Log K	Activation Energy (kj mol^{-1})
Calcite[1]	-5.81 (neutral); -0.3 (acidic); -3.48 (basic)	23.5 (neutral); 14.4 (acidic); 35.4 (basic)
Quartz[1]	-13.40	90.9
Albite[1]	-12.56 (neutral); -10.16 (acidic)	69.8 (neutral); 65.6 (acidic)
Kaolinite[1]	-13.8 (neutral); -11.31 (acidic)	22.2 (neutral); 65.9 (acidic)
Halite[1]	-0.21	7.4
K-Feldspar[1]	-12.41 (neutral); -10.06 (acidic)	38.0 (neutral); 51.7 (acidic)
Enstatite[1]	-12.41 (neutral); -9.02 (acidic)	80.0 (neutral and acidic)
Biotite (with Li^+)[1]	-12.55 (neutral); -9.84 (acidic)	22.0 (neutral and acidic)
Chlinochlore-14A (with Li^+)[2]	-10.32 (neutral); -4.0(acidic); -8.82 (basic)	13.0 (neutral); 30.0 (acidic); 15 (basic)

2.6 Geothermal Power and Lithium production

After one million years, an injection well was placed at 1,100 m and a production well 1,220 m distance from the western boundary (adjacent to the easternmost faults) at elevations 600 m MSL and 200 m from the front face of the model domain (Figure 4B). The wells were activated for thirty years with a pumping rate of 120 kg s^{-1}. Net Energy (Q_{net}) (Equation 1 and 2) generated over thirty years was calculated assuming a reinjection temperature of 80°C, a thermal efficiency rate (e_t) of 12% (Zarrouk and Moon, 2014), and a pumping efficiency rate (e_p) of 20% (Franco and Villani, 2009). Thermal energy rate Q was calculated as a function of pumping rate (M, kg s^{-1}), specific heat of the production water (C, kj kg^{-1} °C^{-1}) at time (t), and the temperature difference between produced and reinjected water (ΔT, °C).

$$Q = MC\Delta T \tag{1}$$

$$Q_{net} = Qe_te_p \tag{2}$$

3. RESULTS

3.1 Model A

Initial simulations without connecting faults showed majority west to east horizontal flow and limited vertical flow. When faults were included in the model domain, flow and heat transport through the faults was evident within 4,000 years, with the western faults indicating flow vertically down and the eastern faults vertically up towards the surface. Within 25,000 years, water greater than 200°C was present around the eastern faulted zones in the upper 400 m of the basin fill aquifer. As the simulation progressed however, the flow direction within each of the four faults, which was initially downward for the two to the west and upward for the two to the east as suggested in the conceptual model (Figure 2) continued to shift as denser, cooler water moving down the faults interfered with the previous movement of hot water vertically upward. While there was consistently hot water transported up and cool water transported down through the faults, which faults were hotter versus cooler was not constant throughout the simulation even up to 1 million years of run time. This pattern of slowly shifting heat distribution continued into 2 million years, but heat did become more established on the eastern side of the graben within the last 25,000 years (Figure 4A). We consider therefore that while the exact location of hot water moving upward through the faults is variable over longer time scales, the simulations do indicate consistent presence of hot water potentially useful for geothermal power (between 150° to greater than 200°C) on human time scales in the shallow regions of the basin fill aquifer on the east side of the graben. Additionally, as suggested by the literature and the conceptual model, vertical movement of the hot water is facilitated by the faults, which penetrate through the igneous layer, indicating that if Li^+ is present in that layer due to dissolution of lithium-bearing minerals, it might also be transported to the shallow subsurface.

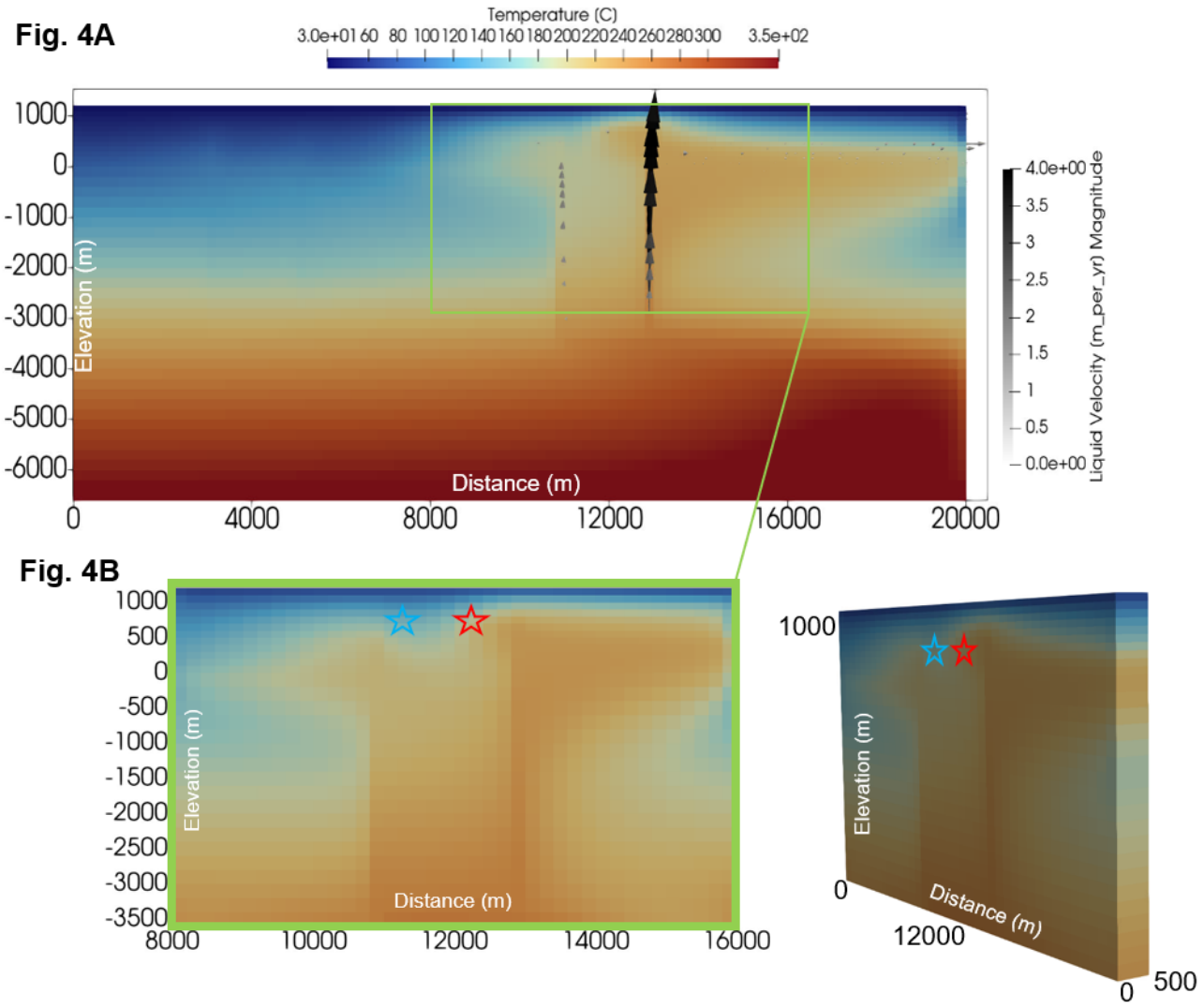

Figure 4A. 2D large-scale flow and heat transport model run for 2 million years and 4B. 3D zoomed in model used for reactive transport and 30 years of geothermal pumping. Production and injection well locations are shown as red and blue stars projected on the front face of the model domain.

3.2 Model B

Primary mineral dissolution and secondary mineral precipitation processes reached equilibrium within 100,000 years of model run-time, after which concentrations remained generally constant (Figure 5). Li-bearing biotite dissolution was followed by Li-bearing chlorite and Li-bearing muscovite precipitation, along with non-Li-bearing chlorite, muscovite, kaolinite, and small quantities of quartz and calcite in the volcanic material and the lower basin fill (Figure 5). Li^+ concentration in solution increased along with biotite dissolution and chlorite and muscovite precipitation, suggesting that these are reasonable potential mechanisms by which Li^+ may be integrated into clay as well as concentrate in the subsurface in the aqueous phase.

From 1.0 x 10^{-8} mol L^{-1}, aqueous Li^+ concentration increased in the subsurface up to a maximum of 1.5 x 10^{-5} mol L^{-1} (0.1 ppm) which, while a definite increase, remains two orders of magnitude short of literature values 2.6 – 5.9 x 10^{-3} mol L^{-1} (15-41 ppm) (Turk et al. 1973). As well, Li^+ concentration was highest in the igneous zone and where cooler water (less than 150°C) was present (Figure 5A). Where water at temperatures useful for geothermal power production was present in the basin fill (150° to >200°C), aqueous Li^+ concentration reached a maximum of 1.0 x 10^{-5} mol L^{-1} and was generally lower (Figure 5B).

Wells were emplaced in the basin fill where there was a good conflux of heat and Li^+ concentration (Figure 4B, Figure 5A) and pumped at a rate of 120 kg s^{-1}. Over thirty years, production well temperature decreased from 215°C to 155°C. Assuming a reinjection temperature of 80°C, a thermal efficiency rate of 12% (Zarrouk and Moon, 2014) and a pumping efficiency rate of 20% (Franco and Villani, 2009), net energy production decreased from 6.8 to 3.9 megawatts (MW) (Figure 6). Total quantity of Li^+ extracted over thirty years was calculated as 777 kg (Figure 7). For comparison, an estimate of the Li^+ brine concentration at the Salton Sea is 200 ppm, with an estimated potential annual extraction of 24,000 metric tons (mt) (Warren, 2021).

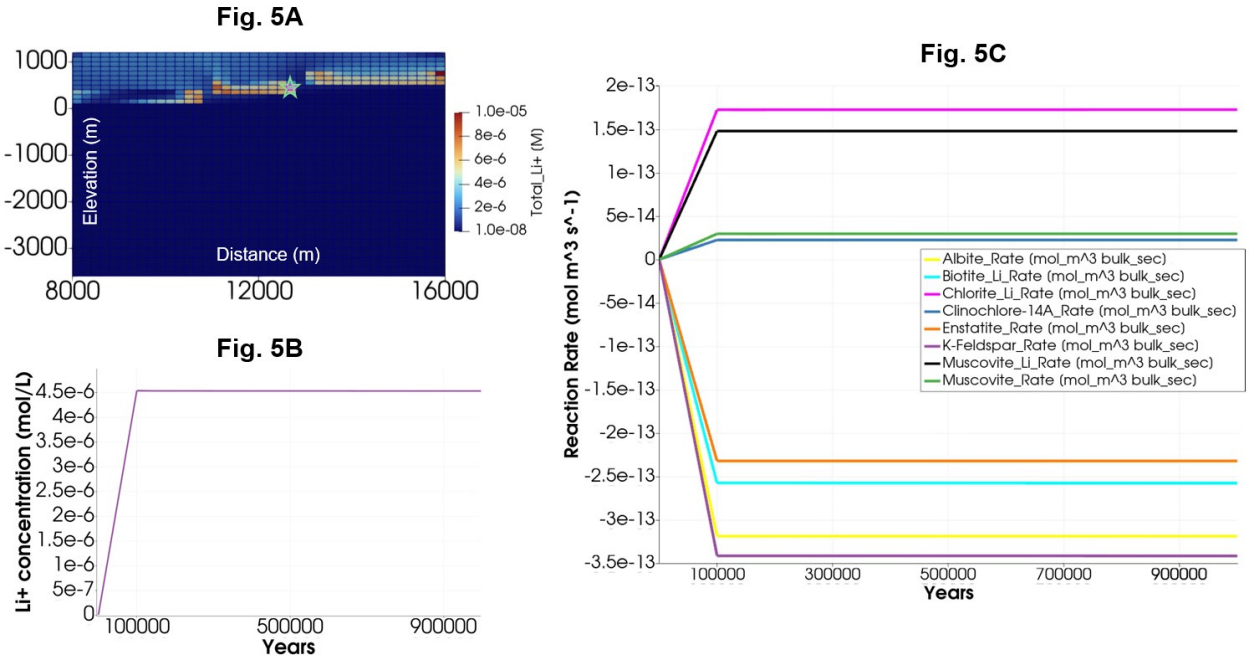

Figure 5A. Li^+ concentration in the subsurface after 1 million years of model run time. Figure 5B. Time series of Li^+ concentration at a select point (green star) in the igneous layer. Figure 5C. Time series of mineral reaction rates at a select point (green star) in the igneous layer, indicating dissolution of silicates and precipitation of clays, reaching steady state after 100,000 years.

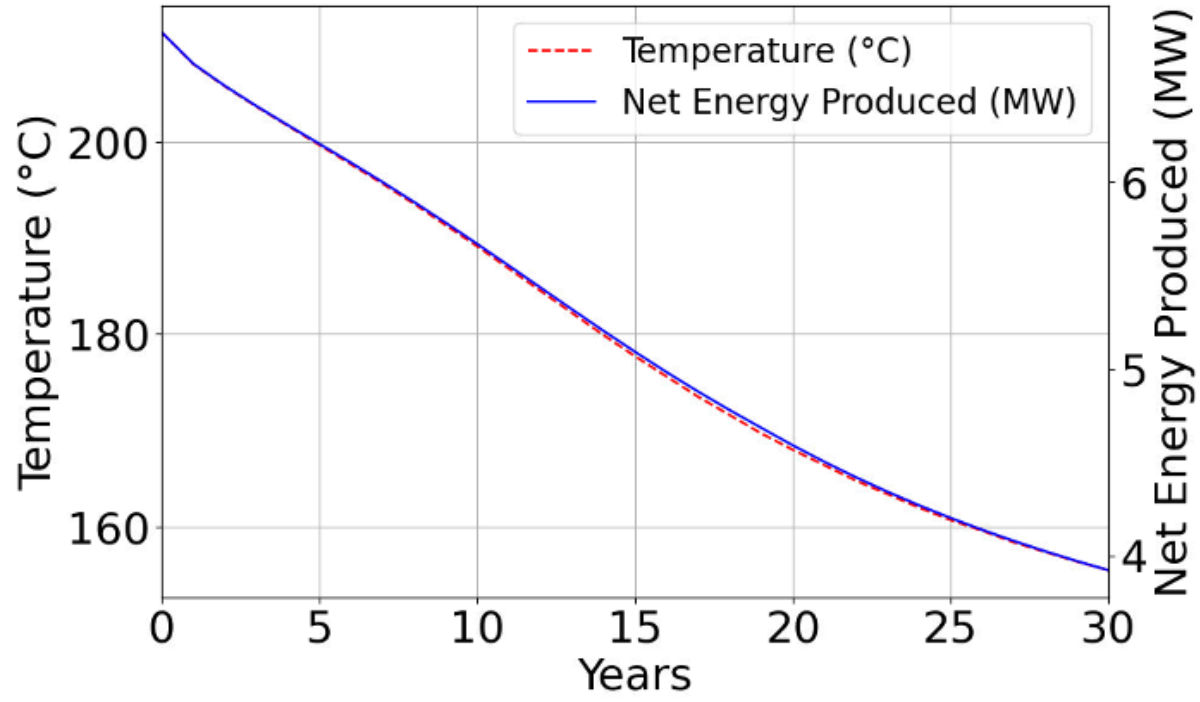

Figure 6. Temperature and net energy production for a hypothetical binary-type geothermal power plant.

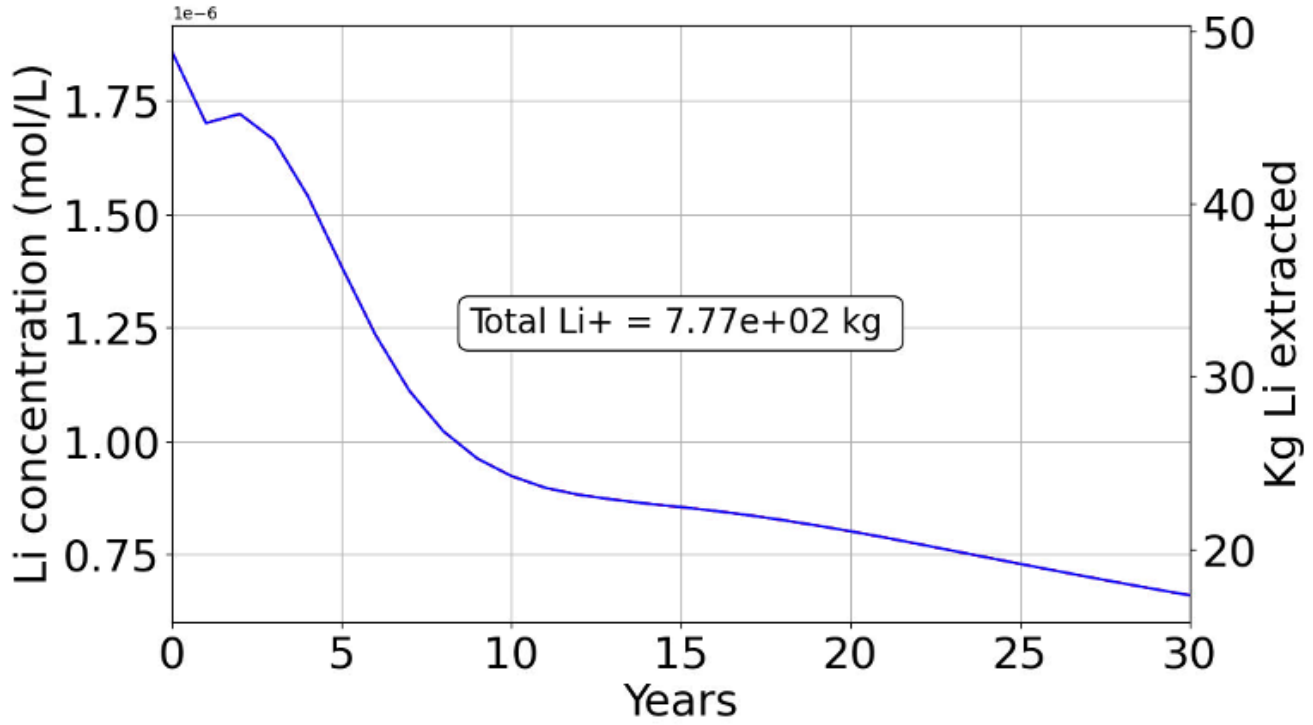

Figure 7. Li^+ co-production from geothermal pumping over 30 years.

4. DISCUSSION

The flow and heat-transport simulations showed variation in flow pattern over the million-year timescale, specifically which side of the graben and which fault had upward flow and which had downward flow. These results differ slightly from earlier conceptual models, which suggested a steady state of cold water down one side of the graben and hot water up the other (Smith et al. 2011) once a stable flow regime established. We suggest that this difference may be due to the distance between faults (~3,000 m), and the fault depth, which does not penetrate beyond -3,600 m below MSL, with initial subsurface temperature of 250°C. Under these conditions, the cooler water moving down one fault is unable to be re-heated to reservoir temperatures before encountering the base of the next fault, mixing, and causing variation in density until a new dominant flow pattern emerges. On the ten-thousand-year timescale, however, flow patterns were relatively consistent, suggesting that 1) vertical heat transport along the graben faults from the carbonate aquifer to the basin fill is a reasonable mechanism for moving heat from depth into the shallower basin fill where it could be used for geothermal power production and 2) if there is dissolution of Li-bearing minerals in the igneous layer, Li^+ might also move into the basin fill, concurrent with the heat. Future work involving a sensitivity analysis on the local thermal gradient, suggested between 35° - 60°C km^{-1} (Smith et al., 2011) and potential reservoir temperatures, will improve understanding of the subsurface heat flow. As well, obtaining more recent data relating to horizontal and vertical permeability of all materials in Wendover Graben, including fault depth, location, and aperture width, would better constrain the simulation and reduce uncertainty concerning whether the long-term flow patterns observed in the simulations are indeed reflective of current subsurface processes at Wendover Graben.

When geochemistry was introduced in Model B, dissolution of Li-bearing biotite in the igneous layer was followed by precipitation of Li-bearing chlorite and Li-bearing muscovite in the igneous layer as well as increased Li^+ concentration in the aqueous phase. The aqueous phase Li^+ moved into the basin fill as suggested by the conceptual model, although concentration remained 2-3 orders of magnitude below that recorded in the literature (Goode, 1978; Turk et al., 1973). When geothermal pumping was simulated, co-extracted quantities of Li^+ were orders of magnitude below Li^+ suggested to be removed from other regions, such as the Salton Sea (Stringfellow and Dobson, 2021; Warren, 2021). We suggest two main reasons for these differences: 1) lack of recent data relating to Li-specific mineralogy at Wendover, particularly the proportion of Li in primary igneous minerals, clays, and volcanic glass, and their location and specific reaction rates and 2) we did not simulate more recent (10-20,000 years) evaporative processes associated with post-Pleistocene shrinking of Lake Bonneville, which is responsible for development of the Bonneville Salt Flats (Mason and Kipp, 1998; Turk et al., 1973), and a major contributor to high salinity in the shallow groundwater.

As the results from the reactive transport model suggest that an additional source of Li^+ other than what can be derived from dissolution of a single lithium bearing mineral phase is likely necessary to bring Li^+ concentration closer to levels reported in the literature (15-41 ppm), upcoming simulations will consider additional potential lithium bearing mineral phases and volcanic glass, the proportion of lithium in these phases, and reaction rates. While the evaporative processes were not included in the model to focus on Li^+ presence in the deeper aquifer where geothermal pumping might take place, it is possible that some degree of mixing between cold, high salinity, high Li^+,

shallow waters and deeper, hotter waters may also increase Li^+ concentration at depth. To investigate this and further constrain the simulations, new well data from Wendover Graben investigating Li^+ occurrence and concentrations at a variety of depths and distances across the graben are planned to further improve the simulations and our understanding of the geochemical processes in the subsurface. In addition, future planned work on this project will incorporate reaction rates from geochemical experiments on volcanic glass and materials from Wendover to better constrain the geochemistry.

5. CONCLUSION

Reservoir simulations were able to demonstrate a flow and heat transport patterns along vertical faults in the Wendover Graben. When reactive transport was included, dissolution of primary igneous minerals and precipitation of secondary Li-bearing clay was present in the igneous layers, and concentration of aqueous Li^+ increased in both the igneous layer and the superjacent basin fill. These results support the possibility for co-production of Li^+ and geothermal power at Wendover Graben. However, Li^+ concentrations were still dilute compared to shallow brine well data, with lower concentrations correlating with higher temperature. These results suggest that other processes such as long-term, repetitive evaporation of Lake Bonneville, may be responsible for concentrating Li^+ sourcing from igneous materials. Geothermal wells, which would be emplaced deeper than the shallow brine in order to access requisite heat, would therefore extract more limited quantities of Li^+ during production than otherwise suggested if only concentrations in the shallow, colder aquifer are considered. Additional data, particularly relating to the geochemistry and temperatures at depth, are needed from Wendover Graben to better constrain the simulations. Following, the broader context of costs associated with lithium extraction and processing, particularly whether the quantity of lithium extracted justifies the processing expense, would need to be taken into consideration when considering Wendover Graben as a potential site for lithium and geothermal co-extraction.

ACKNOWLEDGEMENTS

The work presented in this paper was funded by the U.S. Department of Energy, Geothermal Technologies Office.

This paper describes objective technical results and analysis. Any subjective views or opinions that might be expressed in the paper do not necessarily represent the views of the U.S. Department of Energy or the United States Government.

Sandia National Laboratories is a multimission laboratory operated by National Technology and Engineering Solutions of Sandia LLC, a wholly owned subsidiary of Honeywell International Inc., for the U.S. Department of Energy's National Nuclear Security Administration.

SAND2026-16603C

6. REFERENCES

Benson, T.R., Coble, M.A., Dilles, J.H., 2023. Hydrothermal enrichment of lithium in intracaldera illite-bearing claystones. Science Advances 9, eadh8183. https://doi.org/10.1126/sciadv.adh8183

Carena, S., Friedrich, A.M., 2018. Vertical-displacement history of an active Basin and Range fault based on integration of geomorphologic, stratigraphic, and structural data. Geosphere 14, 1657–1676. https://doi.org/10.1130/GES01600.1

Decarreau, A., Vigier, N., Pálková, H., Petit, S., Vieillard, P., Fontaine, C., 2012. Partitioning of lithium between smectite and solution: An experimental approach. Geochimica et Cosmochimica Acta 85, 314–325. https://doi.org/10.1016/j.gca.2012.02.018

Dobson, P., Araya, N., Brounce, M., Busse, M., Camarillo, M.K., English, L., Humphreys, J., Kalderon-Asael, B., McKibben, M., Millstein, D., Nakata, N., O'Sullivan, J., Planavsky, N., Popineau, J., Renaud, T., Riffault, J., Slattery, M., Sonnenthal, E., Spycher, N., Stokes-Draut, J., Stringfellow, W., White, M., Dobson, P., Araya, N., Brounce, M., Busse, M., Camarillo, M.K., English, L., Humphreys, J., Kalderon-Asael, B., McKibben, M., Millstein, D., Nakata, N., O'Sullivan, J., Planavsky, N., Popineau, J., Renaud, T., Riffault, J., Slattery, M., Sonnenthal, E., Spycher, N., Stokes-Draut, J., Stringfellow, W., White, M., 2023. Characterizing the Geothermal Lithium Resource at the Salton Sea (LBNL Report No. LBNL-2001557). Lawrence Berkeley National Lab.

Forbes, B., Moore, J.N., Finnila, A., Podgorney, R., Nadimi, S., McLennan, J., 2019. Natural fracture characterization at the Utah FORGE EGS test site—discrete natural fracture network, stress field, and critical stress analysis (Miscellaneous Publication No. 169-N). Utah Geological Survey.

Franco, A., Villani, M., 2009. Optimal design of binary cycle power plants for water-dominated, medium-temperature geothermal fields. Geothermics 38, 379–391. https://doi.org/10.1016/j.geothermics.2009.08.001

Frederick, J., Gatz-Miller, H., Lowry, T., 2025. Introducing PFLOTRAN's New Geothermal Fracture Model for Simulation of Geothermal Systems, in: PROCEEDINGS, 50th Workshop on Geothermal Reservoir Engineering. Stanford, California.

Glanzman, R.K., McCarthy, J.H., Rytuba, J.J., 1978. Lithium in the McDermitt caldera, Nevada and Oregon. Energy 3, 347–353. https://doi.org/10.1016/0360-5442(78)90031-2

Goode, H.D., 1978. Thermal Waters of Utah (Topical Report No. DOE/ET/28392-7). Utah Geological and Mineral Survey, Salt Lake City, UT.

Hammond, G.E., Lichtner, P.C., Mills, R.T., 2014. Evaluating the performance of parallel subsurface simulators: An illustrative example with PFLOTRAN. Water Resources Research 50, 208–228. https://doi.org/10.1002/2012WR013483

Jancsek, K., Janovszky, P., Galbács, G., Tóth, T.M., 2023. Granite alteration as the origin of high lithium content of groundwater in southeast Hungary. Applied Geochemistry 149, 105570. https://doi.org/10.1016/j.apgeochem.2023.105570

Kim, K.Y., 1985. Seismic Studies near Crater Island in the Great Salt Lake Desert, Utah (Master's Thesis). University of Oklahoma, Norman, OK.

Lee, K.J., You, J., Gao, Y., Terlier, T., 2024. Release, Transport, and accumulation of lithium in shale brines. Fuel 356, 129629. https://doi.org/10.1016/j.fuel.2023.129629

Lichtner, P., Hammond, G.E., Lu, C., Karra, S., Bisht, G., Benajmin, A., Mills, R., Jitendra, K., 2015. PFLOTRAN User Manual: A Massively Parallel Reactive Flow and Transport Model for Describing Surface and Subsurface Processes.

Mason, J.L., Kipp, K.L., 1998. Hydrology of the Bonneville Salt Flats, northwestern Utah, and simulation of ground-water flow and solute transport in the shallow-brine aquifer (Professional Paper No. 1585), Professional Paper. U. S. Geological Survey. https://doi.org/10.3133/pp1585

Mends, E.A., Chu, P., 2023. Lithium extraction from unconventional aqueous resources – A review on recent technological development for seawater and geothermal brines. Journal of Environmental Chemical Engineering 11. https://doi.org/10.1016/j.jece.2023.110710

Palandri, J.L., Kharaka, Y.K., 2004. A Compilation of Rate Parameters of Water-Mineral Interaction Kinetics For Application To Geochemical Modeling (Open File No. 2004–1068). U. S. Geological Survey, Menlo Park, California.

Smith, M.M., Carroll, S.A., 2016. Chlorite dissolution kinetics at pH3–10 and temperature to 275°C. Chemical Geology 421, 55–64. https://doi.org/10.1016/j.chemgeo.2015.11.022

Smith, R.P., Breckenridge, R.P., Wood, T.R., 2011. Preliminary Assessment of Geothermal Resource Potential at the UTTR (No. INL/EXT-11-22215). Idaho National Laboratory.

Stringfellow, W.T., Dobson, P.F., 2021. Technology for the Recovery of Lithium from Geothermal Brines. Energies 14, 6805. https://doi.org/10.3390/en14206805

Sweetkind, D.S., Cederberg, J.R., Masbruch, M.D., Buto, S.G., 2011a. Hydrogeologic framework, chap. B of Heilweil, V.M., and Brooks, L.E., eds., Conceptual model of the Great Basin carbonate and alluvial aquifer system (Scientific Investigations Report No. 2010–5193). U. S. Geological Survey.

Sweetkind, D.S., Masbruch, M.D., Heilweil, V.M., Buto, S.G., 2011b. Groundwater Flow, chap. C of Heilweil, V.M., and Brooks, L.E., eds., Conceptual model of the Great Basin carbonate and alluvial aquifer system (Scientific Investigations Report No. 2010–5193). U. S. Geological Survey.

Thomas, J.M., Mason, J.L., Crabtree, J.D., 1986. Ground-water levels in the Great Basin region of Nevada, Utah, and adjacent states (USGS Numbered Series No. 694), Hydrogeologic Atlas. U. S. Geological Survey.

Turk, L.J., Davis, S.N., Bingham, C.P., 1973. Hydrogeology of Lacustrine Sediments, Bonneville Salt Flats, Utah. Economic Geology 68, 65–78. https://doi.org/10.2113/gsecongeo.68.1.65

Victor M. Heilweil, L.E.B., 2011. USGS Scientific Investigations Report 2010–5193: Conceptual Model of the Great Basin Carbonate and Alluvial Aquifer System (U.S. Geological Survey Scientific Investigations Repor No. 2010–5193). U.S. Geological Survey.

Warren, I., 2021. Techno-Economic Analysis of Lithium Extraction from Geothermal Brines (Technical Report No. NREL/TP-5700-79178). National Renewable Energy Laboratory.

Whelan, J.A., Petersen, C., 1976. Lithium Sources of Utah, in: Lithium Resources and Requirements by the Year 2000, Geological Survey Professional Paper 1005. U. S. Geological Survey, Golden, CO.

Zarrouk, S.J., Moon, H., 2014. Efficiency of geothermal power plants: A worldwide review. Geothermics 51, 142–153. https://doi.org/10.1016/j.geothermics.2013.11.001

Zhou, J., Wang, Q., Wang, H., Ma, J., Zhu, G., Zhang, L., 2025. Pegmatite lithium deposits formed within low-temperature country rocks. Nature Communications 16, 447. https://doi.org/10.1038/s41467-024-55793-8